

The effect of molecular imprinting on the pore size distribution of polymers

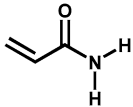
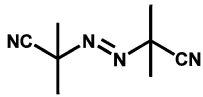
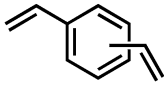
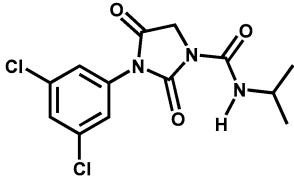
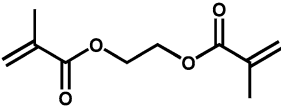
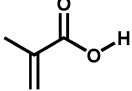
Mohammad Al Kobaisi · Margaret Tate · Colin Rix · Timur S. Jakubov · David E. Mainwaring

Received: 16 April 2007 / Revised: 7 August 2007 / Accepted: 24 September 2007 / Published online: 18 October 2007
© Springer Science+Business Media, LLC 2007

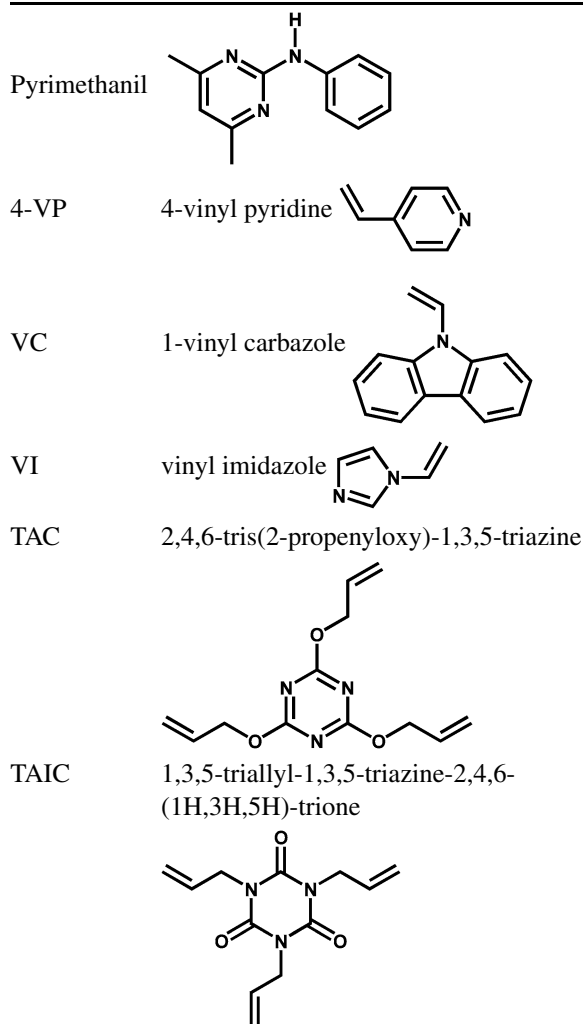
Abstract Molecular imprinting techniques are becoming an increasingly important domain of porous polymers generally, to achieve molecule specific recognition through morphology or stereochemistry of cavities. Imprinting is sought to increase both selectivity and sensitivity where the polymer may be present as particulate, membrane or thin film forms. Here, we detail mechanisms involved in the formation, stability and adsorption of binding sites, through the influence of polymerisation conditions and templates on the porosity of highly crosslinked molecularly imprinted polymers (MIPs). Environmental control represents an important area for porous polymers, here we focus on two template fungicides, iprodione and pyrimethanil, for ethylene glycol dimethacrylate (EGDMA) based polymers. In general, control of the pre-polymerisation interactions were able to vary the surface areas of polymers from 40–60 m² g⁻¹ to 300–436 m² g⁻¹ while pore sizes fell into distributions (a) close to the micropore region at ~3.8 nm, (b) in the 10 to 20 nm mesopore region and (c) in the 20 to 50 nm mesopore region. The importance of intermolecular interactions and aggregation in the pre-polymerisation solution to the Brunauer, Emmett, Teller (BET) surface areas and pore size distribution of final polymers has been demonstrated by systematic variation of chemical functionality. These effects confirm recent molecular dynamic simulation studies of MIP formation and cavity stability.

Keywords Biochemical, energy and environmental applications · Fundamentals of adsorption · Liquid phase adsorption

Abbreviations

ACM	acrylamide	
AIBN	α, α' -azoisobutyronitrile	
D	pore diameter	
DVB	divinylbenzene	
GCMC	Grand Canonical Monte Carlo	
Iprodione		
EGDMA	ethylene glycol dimethacrylate	
MAA	methacrylic acid	
NIP	non-imprinted polymer	
P	pressure (Pa)	
P ₀	saturated pressure (101325 Pa)	
P/P ₀	relative pressure	

M. Al Kobaisi · M. Tate · C. Rix · T.S. Jakubov (✉) · D.E. Mainwaring
School of Applied Sciences, Royal Melbourne Institute of Technology, Melbourne 3001, Australia
e-mail: timur.jakubov@rmit.edu.au



1 Introduction

Porous polymers, formed by a diverse range of techniques, have become an important cornerstone in many advanced materials with enhanced functionality. Applications of these materials range across chemical and biological separation media and membranes, polymer electrolytes in energy storage systems, templates for nanomaterial synthesis and sensing technologies. Pores in these biphasic materials, span macropores (>50 nm), mesopores (2–50 nm) and micropores (<2 nm). Increasingly research interest lies in nanoporous materials having pores in the range less than 50 nm but importantly macroporosity above 50 nm provides much of the connective and mass transport in such systems. Recently formation techniques and applications of nanoporous polymers have been extensively reviewed (Raman and Palmese 2006). Among the synthesis techniques gaining increased attention, molecular imprinting relies on the co-polymerization of a functional monomer with a cross-linking counterpart in the presence of a targeted template

molecule. Assembly of a supramolecular complex prior to polymerisation and the subsequent removal of the template has formed the basis of MIPs showing molecular recognition characteristics attributed to the presence of these imprinted binding sites. Ulbricht and Malaisamy (2005) have related the final interstitial porosity to both the polymer phase inversion and particle morphology during MIP membrane formation while Yoshimatsu et al. (2007) have related it to particle morphology. Several studies on the synthesis and molecular recognition of MIPs have reported both particle size and morphology as well as pore sizes (Strikovskiy et al. 2003; Lin et al. 2006; Liu et al. 2006). Recently Yungerman and Srebnik (2006) have examined the effectiveness of cross-linked polymer networks as MIPs through molecular dynamic simulation before and after template removal.

Further detailed understanding of many of the mechanisms involved in the formation, stability and heterogeneity of the adsorption and binding sites remains. One of the least studied aspects has been the microstructure and stability of the binding cavities within the porous polymer network. Here, we examine the influence of polymerisation conditions as well as the presence of templates on the porosity of a MIP highly crosslinked to minimize swelling behaviour and maintain integrity of the adsorption-rebinding space. The fungicides, iprodione and pyrimethanil, were used as templates to imprint EGDMA based polymers to study the effect of the presence of these templates. Detailed analysis of the pore size distribution of polymers, with and without imprinting with iprodione and pyrimethanil, using a series of functional monomers monitored the association strength within the pre-polymerisation complex between the template and the functional monomer.

2 Experimental

2.1 Reagents

Organic solvents used in syntheses were spectrophotometric grade ($\geq 99.5\%$) and water used was deionised. The following compounds were used: α, α' -azoisobutyronitrile ($\geq 98\%$ GC); iprodione (98%); pyrimethanil (98%); ethylene glycol dimethacrylate, EGDMA (50% GC, Fluka); methacrylic acid, MAA ($\geq 98\%$, Aldrich); 4-vinyl pyridine, 4-VP (95%, Sigma-Aldrich); acrylamide, ACM (99+); 1,3,5-triallyl-1,3,5-triazine-2,4,6-(1H,3H,5H)-trione, TAIC (99% GC, Fluka); 2,4,6-tris(2-propenyloxy)-1,3,5-triazine, TAC (98% GC, Fluka); 1-vinyl carbazole, VC ($\geq 98\%$ GC, Fluka); vinyl imidazole, VI (99%, Sigma-Aldrich) and divinylbenzene, DVB (80% GC, Fluka).

2.2 Preparation of polymers (NIP and MIP)

In a typical MIP synthesis, the polymerisation mixture consisted of solvent, monomers, initiator and the template molecule (iprodione or pyrimethanil). The functional monomer to crosslinker molar ratio was 1:5. The initiator to monomer ratio used was 2% w/w with a solvent ratio of 50% v/v. The template to functional monomer ratio was varied from 1:5 to 1:1. The polymerisation mixture was sparged with nitrogen for 5–10 minutes to remove oxygen prior to commencing the reaction. Polymerisation was initiated by UV irradiation using a 125 W medium pressure mercury lamp in a photochemical reactor for 16 h. Non-imprinted polymers were synthesised in a similar manner, without the addition of the template molecule to the polymerisation solution.

After removal from the polymerisation reaction vessel, the polymers were crushed and ground wet with acetone using a mortar and pestle. Template extraction and removal of unreacted monomers from the templated and non-templated polymers were conducted by extraction using acetone in a Soxhlet apparatus for 72 h. The polymers were then removed and dried at 70 °C. FTIR analyses (Perkin Elmer 2000, USA) with KBr disks of the polymers before and after the extraction process confirmed template removal and polymer structural stability during the extraction procedure.

2.3 Characterisation of polymers

Nitrogen adsorption isotherms were measured at -196°C using an ASAP-2000N adsorption analyser (Micromeritics, USA). Prior to adsorption measurements, each polymer sample (100–150 mg) was degassed at 70 °C under high vacuum for at least 12 h. The total pore volume was calculated by converting the amount of nitrogen adsorbed at a relative pressure of about 0.99 to the volume of liquid adsorbate. Adsorption and desorption isotherms were recorded using an 89-point pressure table with 15 s equilibration intervals.

The surface areas were evaluated using the BET method and the average pore diameter and pore size distribution were calculated using the Barrett, Joyner, Halenda (BJH) analysis of the desorption branch.

3 Results and discussion

3.1 Solvency effect on polymer microstructure

Based on the growth mechanism functioning during the polymerisation process, solvency during polymerisation produces a significant variation in the porosity of the polymer structure. This solvency effect was examined by a comparison of the solvent systems methanol:water and acetonitrile for a series of EGDMA cross-linked polymers as shown in Table 1. Scanning electron microscopy showed that polymers varied from an aggregation of polymer particles to microchannelled, polymer networks. Methanol:water, a non-porogenic solvent, which did solvate the growing polymer network, yielded polymers that had larger macropores in the region 55 to 100 nm formed from irregular voids between clusters of microparticles and relatively lower BET surface areas between 63 to 160 $\text{m}^2 \text{g}^{-1}$. While acetonitrile, a porogenic solvent, produced smaller macropores in the range 60 to 80 nm which were produced by a more regular channel network between individual polymer globules and surface areas that ranged up to 400 $\text{m}^2 \text{g}^{-1}$.

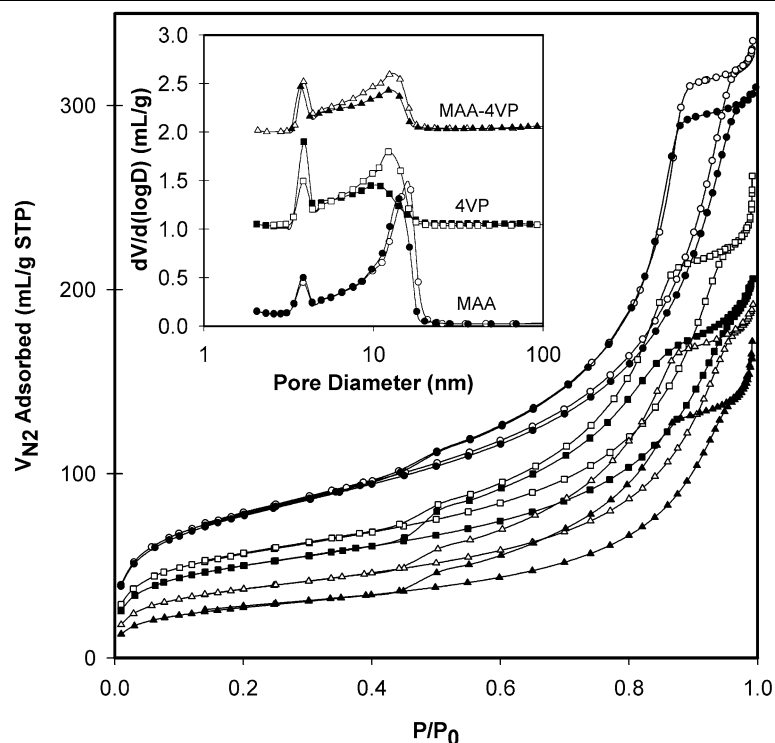
3.2 Effect of the iprodione template on polymer microstructure

Comparative nitrogen adsorption of the non-templated and iprodione templated polymers showed fundamental differences in the pore microstructure. Figure 2 shows a comparison of three systematic polymer systems. The active surface areas of the non-templated EGDMA-MAA and 4VP

Table 1 Summary of active surface area analysis of EGDMA polymers prepared in ACN (MAA, MAA-4VP [1:1] and MAA-4VP [1:3]) and water/MeOH (MAA-4VP [1:1], 4VP, MAA-4VP [1:3]) solvent systems

Solvent system	Polymer			
	MAA	MAA-4VP (1:1)	4VP	MAA-4VP (1:3)
	BET surface area (m^2/g)			
MeOH-water	–	46	155	63
ACN	327	317	–	318
	Micropore area (m^2/g)			
MeOH-water	–	21	57	22
ACN	89	89	–	68
	Micropore volume (mL/g)			
MeOH-water	–	0.009	0.025	0.009
ACN	0.038	0.0037	–	0.028

Fig. 1 Nitrogen adsorption-desorption isotherms and BJH pore size distributions of EGDMA copolymers with (○●) MAA, (□■) 4VP, (△▲) 4VP-MAA (1:1) where open and closed symbols represent non-templated and iprodione templated polymers respectively



polymers provides an insight into the pre-polymerisation arrangement of these functional monomers. MAA self associates via strong H-bonding interactions to form small carboxylic acid dimer species prior to polymerisation while 4VP interacts with itself via π - π ring stacking to form a larger comparatively less stable self-associated species. The surface area of the EGDMA-MAA polymer is 55% greater than the EGDMA-4-VP equivalent (287 and 185 $\text{m}^2 \text{g}^{-1}$ respectively) indicating that the weakly associated 4VP molecules offer a considerably larger steric hindrance to polymer growth i.e. growing polymer networks encounter associated large functional monomers and propagate by accommodating them in confined growth, whereas the comparatively smaller dimeric MAA in solution offers a reduced spatial restriction to chain growth resulting in less confined polymer networks. Figure 1 indicates a primary porosity peak at ~ 3.8 nm for all three systems and a mesoporosity peak of the MAA system at about 15 nm which shifts to about 10 nm for the 4VP system with more confined chain growth. In the case of non-templated EGDMA-MAA-4VP, the weaker association interactions of π - π ring stacking in 4VP are disrupted by stronger acid-base interactions between 4-VP and MAA which will further interrupt the developing polymerisation network growth giving EGDMA-MAA-4VP the lowest surface area of these three non-templated polymers (138 $\text{m}^2 \text{g}^{-1}$).

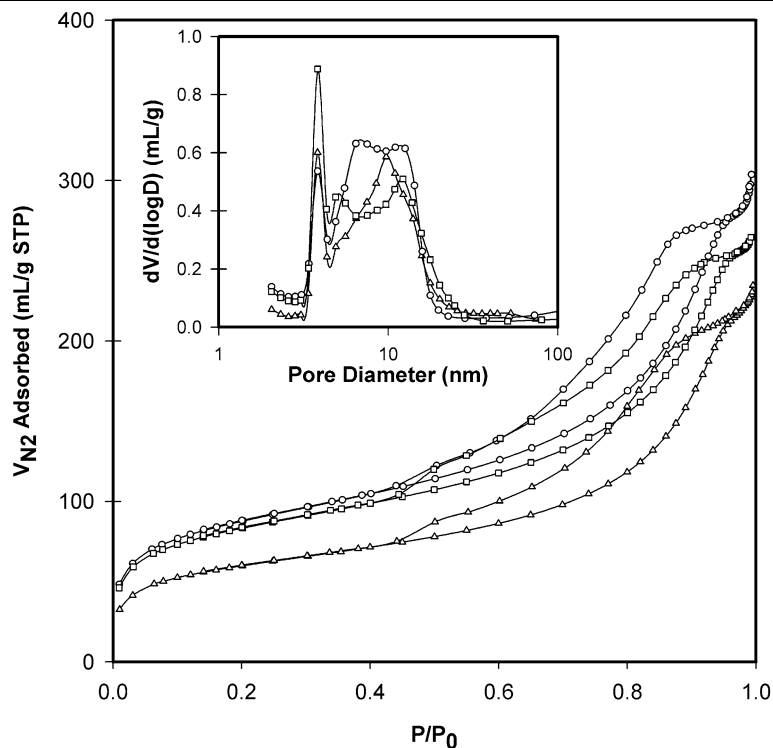
The presence of templating iprodione has little effect on the chain growth in EGDMA-MAA with its small, strongly associated MAA dimers (284 $\text{m}^2 \text{g}^{-1}$), while the presence of

iprodione in the EGDMA-4VP polymer pre-polymerisation mixture disrupts the 4VP interaction through additional π - π ring stacking (pyridyl ring that interacts with the dichlorophenyl ring of the iprodione) which upon template removal increases the surface area from the non-imprinted 185 $\text{m}^2 \text{g}^{-1}$ to 208 $\text{m}^2 \text{g}^{-1}$. In the EGDMA-MAA-4VP system, the acid-base interaction in the pre-polymerisation mixture is very strong, and any interaction between 4VP and iprodione through ring stacking appears to only confine networks more and lower further the surface area to 101 $\text{m}^2 \text{g}^{-1}$.

3.3 Effect of template molecular structure on polymer microstructure

The molecular structure of template molecules influences the polymer microstructure. Here this effect is investigated with the two fungicides iprodione and pyrimethanil, and the polymer system EGDMA-ACM, ACM may act as both a weak base through the carbonyl H-bond acceptor and a weak acid through the amide H-bond donor. The non-templated polymer had a surface area of 217 $\text{m}^2 \text{g}^{-1}$ and a pore size distribution with two peaks consisting of a narrow distribution about 3.8 nm and a wider distribution about 9.6 nm in the mesopore region as shown in Fig. 2. The presence of either template molecule during the formation of the soluble pre-polymerisation complex led to an increase in surface area, here 31% for iprodione and 38% for pyrimethanil compared to the non-templated polymer. The iprodione templated polymer had a surface area of 317 $\text{m}^2 \text{g}^{-1}$ as well

Fig. 2 Nitrogen adsorption-desorption isotherms and BJH pore size distributions of (Δ) non-templated and (\circ) iprodione templated (\square) pyrimethanil templated EGDMA-ACM polymers



as a new peak in the pore size appearing at about 6.4 nm which is indicative of the ability of iprodione to H-bond with the ACM monomer yielding a looser packing of polymer networks, whereas the pyrimethanil templated polymer had a surface area of $301 \text{ m}^2 \text{ g}^{-1}$ and a distinctive peak towards the micropore region at 5 nm. The polymers EGDMA-MAA (Fig. 1) and EGDMA-ACM (Fig. 2) may be compared where it appears that the very weak interaction between MAA and iprodione can not appreciably change the pore size distribution between non-imprinted and imprinted polymers but with EGDMA-ACM, the acrylamide monomer provides both carbonyl and amine groups capable of interacting with the carbonyl and amide groups of the iprodione. Although still weak, these more extensive interactions provide new porosity in a region below 10 nm towards the micropore region.

The impact of the strength of the template–monomer interaction on the polymer microstructure was evaluated by selecting a strongly acidic functional monomer EGDMA-MAA which would provide a strong association with the template pyrimethanil. The impact of solvency on this strong association was also examined by increasing the chloroform content. Table 2 shows the non-imprinted polymer had pores in the region of 3.8 nm together with a broad group of pores with diameters between 4 and 10 nm and a surface area of $291 \text{ m}^2 \text{ g}^{-1}$, while the templated polymer produced only one distribution of pores at about 3.8 nm, no broad peak of larger pores and a surface area of $249 \text{ m}^2 \text{ g}^{-1}$. Increasing the solvent ratio of the system produced narrower, higher, peaks

in the distribution, shifted slightly to lower pore sizes. Increased solvent ratio also increased the surface areas of both the non-templated and templated polymers by 12% and 8% respectively as may be expected with less tightly packed aggregates.

3.4 Effect of the functional monomer aromaticity on polymer microstructure

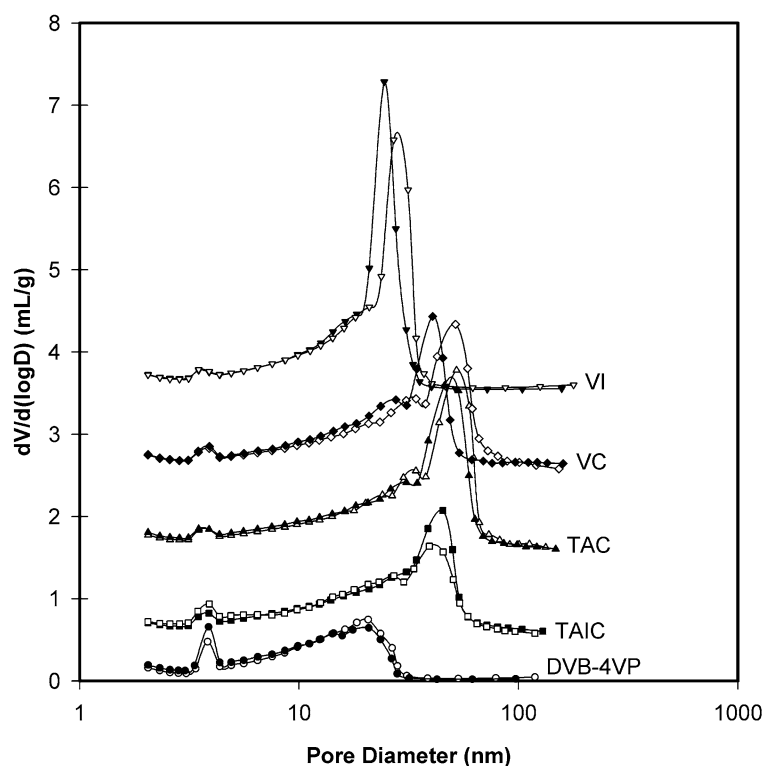
The influence of aromaticity of the functional monomers on the polymer microstructure of non-templated and iprodione templated polymers was investigated by the introduction of a series of heterocyclic aromatic monomers that can participate in π - π ring stacking interactions. This series, consisting of VI, VC, TAC and TAIC, yielded the highest polymer surface areas ranging from $312 \text{ m}^2 \text{ g}^{-1}$ to $436 \text{ m}^2 \text{ g}^{-1}$ as well as the largest pore diameters, 30 nm to 50 nm, and widest pore size distributions for these macropores (Fig. 3). Such pore diameters are characteristic of macropores arising from irregular interstices between clusters of polymer globules. Notably pores with diameters in the range of ~ 3.8 nm were not dominant, indicating that these larger pores are due to high degrees of ring stacking between monomers in both the non-templated and iprodione templated cases.

Finally, the impact of aromaticity and hydrophobicity of the monomers was examined by inclusion of DVB as a co-monomer within the EGDMA-4VP polymer system. Figure 3 shows the EGDMA-DVB-4VP polymer producing mesopores in the region of 3.8 nm similar to EGDMA-4VP as shown in Fig. 1, but with larger mesopores shifted

Table 2 Summary of pore size distribution of EGDMA-MAA polymers prepared in 36% v/v CHCl_3 and 60% v/v CHCl_3 templated for pyrimethanil

		EGDMA-MAA prepared in 36% chloroform		EGDMA-MAA prepared in 60% chloroform	
		NIP	MIP	NIP	MIP
Pore 1	Peak centre (nm)	3.9	3.9	3.8	3.9
	Range (nm) at half peak height	5.2	5.3	6.2	4.8
	Micropore volume (mL g^{-1})	0.364	0.524	0.709	0.699
Pore 2	Peak centre (nm)	6.5	–	4.9	–
	Range (nm) at half peak height	3.8	–	2.1	–
	Micropore volume (mL g^{-1})	1.077	–	0.938	–

Fig. 3 The BJH pore size distribution of
 (○) non-templated and
 (●) iprodione templated
 EGDMA-DVB-4VP polymers,
 (□) non-templated and
 (■) iprodione templated
 EGDMA-TAIC polymers,
 (△) non-templated and
 (▲) iprodione templated
 EGDMA-TAC polymers,
 (◇) non-templated and
 (◆) iprodione templated
 EGDMA-VC polymers and
 (▽) non-templated and
 (▼) iprodione templated
 EGDMA-VI polymers



from about 10 nm to a wider distribution with a peak at about 20 nm. Similar to EGDMA-4VP, template removal increased the small mesopore peak at 3.8 nm, but unlike EGDMA-4VP incorporation of the additional aromaticity of DVB caused the template to have negligible effect on the larger mesoporosity around 20 nm.

4 Conclusions

The influence of polymerisation conditions and the presence of a removable template molecule have been shown to enable a wide spectrum of polymers with varying pore size distributions and surface areas to be synthesized. Analysis

of the resultant porosity and surface areas provides insight into the non-covalent pre-polymerisation arrangement of the functional monomers whose functionality could be varied to influence this soluble precursor complex. These findings showed that:

- hydrogen bonding and aromatic π - π ring stacking were as key interactions between the soluble monomers themselves, and with template molecules, prior to formation of the polymer network, and that strong, dimeric H-bonding (e.g. MAA systems) yielded reduced spatial restriction on the growing polymer networks and produced polymers with surface areas of about $287 \text{ m}^2 \text{ g}^{-1}$. These interactions were independent of template molecules.

- (b) the formation of larger pre-polymerisation π - π ring stacking complexes formed (e.g. 4VP systems) confined polymer network growth, reducing surface areas by about 55% but the presence of template molecules was able to partially ameliorate this reduction.

As well as composition of the pre-polymerisation monomers and template molecules, solvency during the polymerisation phase was also shown to influence both pore size distribution and BET surface areas.

This showed that:

- (c) effective solvating media (methanol:water) produced lower surface area polymers whereas poorly solvating media (acetonitrile) resulted in polymers with comparatively higher surface areas. In general, control of the pre-polymerisation interactions was able to vary the surface areas of polymers from 40–60 m² g⁻¹ to 300–436 m² g⁻¹ while pore sizes fell into (a) distributions close to the micropore region at \sim 3.8 nm, (b) distributions in the 10 to 20 nm mesopore region, and (c) pores in the 20 to 50 nm meso and macropore regions.

It has been shown that BJH analysis of pores approaching the micropore region have a greater disparity in their pore distribution, compared to geometrically Grand Canonical Monte Carlo simulated distributions, than larger mesopores (Gelb and Gubbins 1998). Effects such as seen with the lower reliability of the Kelvin equation for small pores, and the variation of surface tension with very low radii of curvature, were considered in addressing this disparity. With many of the issues relating to the applicability of the Kelvin equation for small confined volumes an active area of adsorption science, porous polymer systems introduce a new complexity in this characterisation, due to the impact of their very varied chemical functionality on wetting and contact

angle behaviour. The influence of pre-polymerisation aggregation on the formation and distribution of pores within the final polymer, as found here, is confirmed by the molecular dynamics study of Yungerman and Srebnik (2006) who, concentrating on template aggregation, found that aggregation occurs prior to polymerisation, and that the local environment of the aggregates had a consistent effect on cavity formation within the extracted polymer.

References

- Gelb, L.D., Gubbins, K.E.: Characterisation of porous glasses by adsorption: models, simulations and data inversion. In: 6th Fundam. of Adsorption Conference, Giens, France, pp. 551–556 (1998)
- Lin, L.-Q., Li, Y.-C., Fu, Q., He, L.-C., Zhang, J., Zhang, Q.-Q.: Preparation of molecularly imprinted polymer for sinomenine and study on its molecular recognition mechanism. *Polymer* **47**, 3792–3798 (2006)
- Liu, X., Ouyang, C., Zhao, R., Shangguan, D., Chen, Y., Liu, G.: Monolithic molecularly imprinted polymer for sulfamethoxazole and molecular recognition properties in aqueous mobile phase. *Anal. Chim. Acta* **571**, 235–241 (2006)
- Raman, V.I., Palmese, G.R.: *Nanomaterials Handbook*, Chap. 21. CRC (2006)
- Strikovskiy, A., Hradil, J., Wulff, G.: Catalytically active, molecularly imprinted polymers in bead form. *React. Funct. Polym.* **54**, 49–61 (2003)
- Ulbricht, M., Malaisamy, R.: Insights into the mechanism of molecularly imprinting by immersion precipitation phase inversion of polymer blends via a detailed morphology analysis of porous membranes. *J. Mater. Chem.* **15**, 1487–1497 (2005)
- Yoshimatsu, K., Reimhult, K., Krozer, A., Mosbach, K., Yei, L.: Uniform molecularly imprinted microspheres and nanoparticles by precipitation polymerization: the control of particle size suitable for different analytical applications. *Anal. Chim. Acta* **584**, 112–121 (2007)
- Yungerman, I., Srebnik, S.: Factors contributing to binding-site imperfections in imprinted polymers. *Chem. Mater.* **18**, 657–663 (2006)